

# Investigation of Processes in the Keyhole of Electron-Beam Welding by Monitoring the Secondary Current Signal in the Plasma

D. N. Trushnikov, V. E. Shchavlev, G. M. Mladenov and L. N. Krotov

**Abstract** An experimental study of the signal patterns of the secondary current in a plasma during electron-beam welding was carried out. The studies show that the spectrum of the secondary emission signal during steel welding has a pronounced periodic component at a frequency of around 15–25 kHz. The signal contains quasiperiodic sharp peaks (impulses). These impulses have a stochastically varying amplitude and follow each other in series, at random intervals between series. The impulses have a considerable current (up to 0.5 A). It was established that during electron-beam welding, the oscillation of the electron beam impulses follow each other almost periodically. It was shown that the probability of occurrence of these high-frequency perturbation increases with the concentration of energy in the interaction zone. This chapter also presents hypotheses for the mechanism of the formation of the high-frequency oscillations in the secondary current signal in the plasma.

**Keywords** Electron-beam welding · Keyhole · Plasma · Beam deflection oscillation

## 1 Introduction

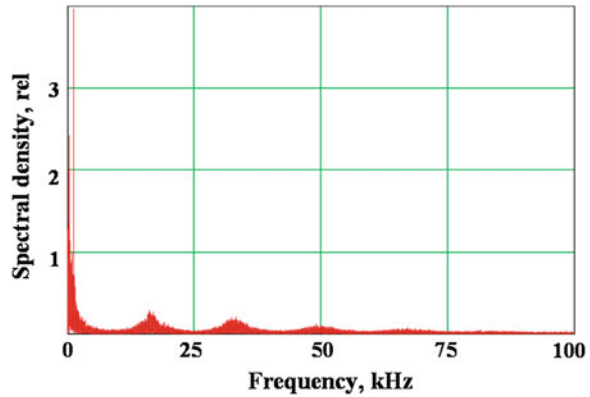
Using electron-beam oscillation to prevent defects during electron-beam welding is widely known. However, there are still no universal methods for regulating the form and parameters of oscillation. Recommendations for the choice of parameters

---

D. N. Trushnikov (✉) · V. E. Shchavlev · L. N. Krotov  
Perm National Research Polytechnic University, Komsomolsky Avenue 29, Perm,  
Russia 614990  
e-mail: trdimitr@yandex.ru

G. M. Mladenov  
Institute of Electronics, Bulgarian Academy of Sciences, Sofia, Bulgaria

**Fig. 1** A typical signal spectrum of the secondary current in the plasma during electron-beam welding with beam oscillation (welding power: 2.5 kW, sharp focus regime ( $\Delta I_f = 0$ ), oscillation frequency: 561 Hz, oscillation size  $-2$   $A = 0.9$  mm)



of oscillation are often contradictory. These problems are due to a lack of knowledge. There are no finished dynamic models describing the processes occurring in the keyhole. The complex character and high speed of these processes make numerical modeling very difficult. All of these mean that additional research into electron-beam welding with an oscillating electron beam are necessary.

This research can be conducted with several aims. It is possible to investigate experimentally the influence of various kinds of oscillation on the forms and quality of a weld [1, 2]. Some articles present the results of research into processes in the keyhole for the parameters of the signal from the secondary current in the plasma during electron-beam welding, which have achieved some success [3–8]. Similar research is well underway for laser welding [9–12]. However, many questions are still outstanding. Most studies have considered the low-frequency range of the secondary signals (2–5 kHz) [3, 5, 6]. However, there are studies showing the probability of occurrence of self-oscillating process with a time constant of  $t \sim 10^{-4}$  s during keyhole welding [13, 14]. These high-frequency processes in the “electron beam-plasma-keyhole” system will be highlighted in this chapter. The chapter also presents hypotheses for the mechanism of formation of high-frequency oscillations in the secondary current signal in the plasma (Fig. 1).

## 2 Experimental Procedure

A ring electrode collector was used to measure the secondary current from the plasma. The collector was located over the zone of welding. The collector has a positive potential of 50 V. The loading resistance was 50  $\Omega$ . The signal from the collector was registered by a data acquisition system and further processed by a computer. The sampling frequency in the experiments was in a range from 100 kHz to 1 MHz per channel.

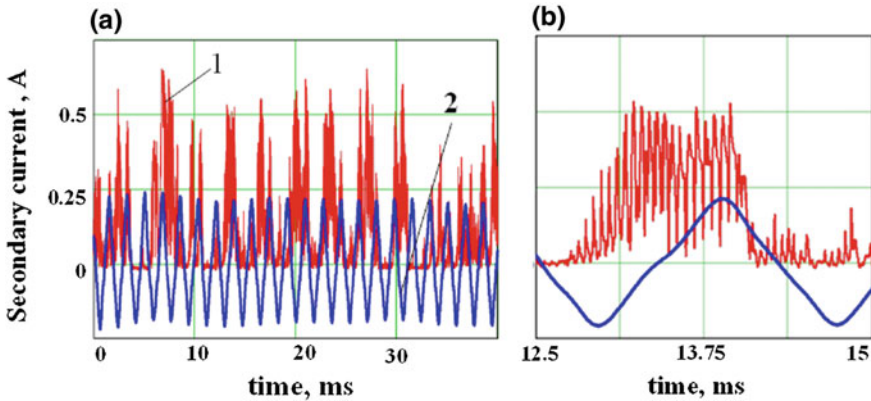


**Fig. 2** Waveform of secondary current in the plasma and the signal of the deflection coil current during electron-beam welding with oscillation across the joint. 1.  $Data(t)$  secondary current. 2.  $Osc(t)$  signal from the deflection coil current

During the experiments, samples of chrome-molybdenum steel (0.15 % carbon, 5 % chrome and around 1 % of molybdenum) and high-alloy chrome-nickel steel (up to 0.12 % carbon, 18 % chrome and up to 0.8 % titanium) were welded. The accelerating voltage in all experiments was 60 kV. The welding power was in the range from 2 to 4 kW.

During the experiments, the welding power  $P$ , focus degree  $\Delta I_f$  ( $\Delta I_f = I_f - I_{f_0}$  is the difference between the focus coil current of the welding mode and the focus coil current of sharp focus), the frequency  $f$  and amplitude of the oscillations  $A$  were varied (Fig. 2).

Beam oscillations across the joint and along the joint were applied. The current in the deflection coils was changed under a linear law. The limits of the beam oscillation frequency were from 90 to 1,500 Hz. The amplitudes of these oscillations were in a range from 0.1 to 1.5 mm for transverse oscillations and from 0.4 to 3.5 mm for oscillations along the joint. Welding speed was 5 mm/s, residual pressure in the vacuum chamber was  $10^{-2}$  Pa. The partial penetration mode took place in experiments.

Transverse metallurgical sections of the weld were made from all the welded samples. The focus regime was determined by the transverse sizes of the penetration depth. The sharp focus regime corresponds to the maximum penetration depth.

In the given work, research into the secondary signal was conducted using coherent accumulation, which is an enhancement of coherent detection, and is widely applied to tracking an electronic beam on a seam, but it has been applied to research processes in the keyhole and welding control only recently. In this research, the high-frequency range 15–20 kHz was studied.

The coherent accumulation method is illustrated in Fig. 3. The small-width square-wave signal is formed from the signal from the current of the deflection coils ( $Osc(t)$ ) less a basic signal  $g(t)$ . The basic signal  $g(t + \tau)$  is shifted relative to the initial signal  $Osc(t)$  for a set time  $\tau$ .

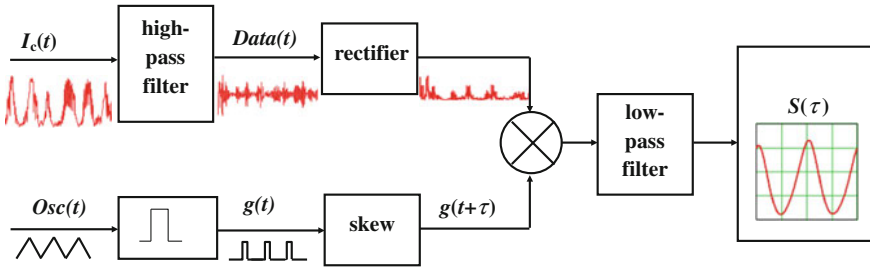


Fig. 3 Coherent accumulation method

### 3 Results and Discussion

Figure 1 shows a typical spectrum of the secondary current signal in a plasma during welding of steel samples. It can be noted that there is a characteristic maximum in the signal at frequencies close to 15 kHz. Figure 2a shows the secondary signal together with a signal of rejecting deflection coils. The processes in the keyhole become periodic with beam oscillations. Frequency perturbations in the secondary current start to periodically follow at multiples of the oscillation frequency. More detailed consideration (Fig. 2b) shows that each perturbation represents a series of high-frequency quasiperiodic impulses. Their frequency 10–25 kHz is very stable for different materials. The amplitude changes randomly. The spectrums and waveforms of the secondary current in a plasma during electron-beam welding are more fully described in [4, 7, 15, 16]. Further studies are planned on the dependence of the frequency of the pulses from the welded materials.

The signal of the secondary current in the plasma  $I_c(t)$  is processed by a digital or analog high-pass filter with a cutoff frequency around 10 kHz. The selected signal of the high-frequency component ( $Data(t)$ ) is rectified and then multiplied by the basic signal,  $g(t + \tau)$ . The result is integrated over time. As a result, we have the function  $S(\tau)$

$$S(\tau) = \int_0^{t_0} g(t + \tau) \cdot |Data(t)| dt, \quad (1)$$

where  $t_0$  is the sampling time. This function  $S(\tau)$  expresses the average amplitude of the high-frequency secondary signal for each value of the shift  $\tau$ .

In other words, there is an area of interaction of the beam with the metal on the keyhole wall, which can be described as the area of maximum power allocation. In the oscillation process of the electron beam, this area moves around the walls of the keyhole. In each position, there is an average value of the amplitude of the high-frequency oscillations of the secondary signal.

Figure 4 shows the results of processing the secondary current signal using coherent accumulation with oscillation across a joint. The sharp focus regime was

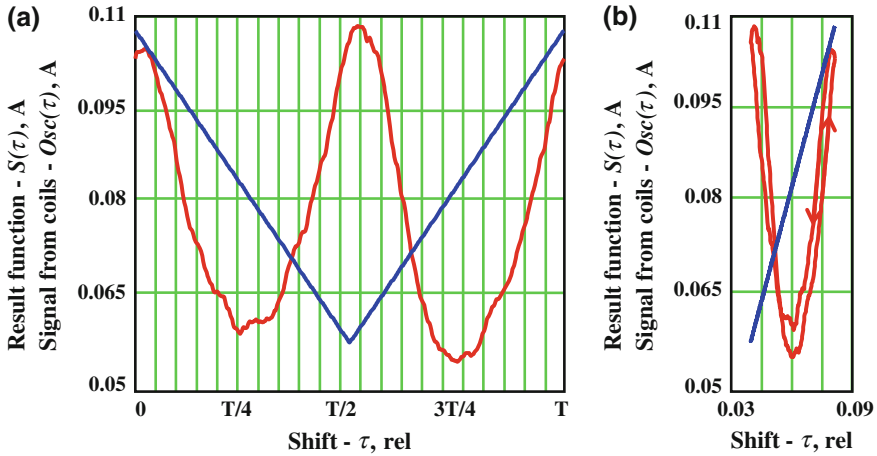


**Fig. 4** Function  $S(\tau)$ , obtained using the coherent accumulation method on  $\tau$ , is the result of secondary processing of the high-frequency component signal.  $Osc(\tau)$  is the record of the deflection coil current ( $P = 2.5$  kW, sharp focus ( $\Delta l_f = 0$  mA), oscillation frequency  $f = 561$  Hz, sweep size  $2A = 1$  mm)

used. The frequency was 560 Hz and the sweep size was 1 mm. It is noticeable that the function is almost symmetric, as, probably, expected. It is possible to present this function in phase space. For this purpose, on a horizontal axis we postpone the current of the deflection coils or the displacement of the electron beam in the keyhole (Fig. 5b).

Figure 5 shows the results for longitudinal oscillation. The asymmetry of the figure for longitudinal oscillations reflects the asymmetry of the keyhole in the longitudinal direction. In the secondary signal spectrum in this case the first harmonic of the signal will prevail. The characteristic lag of the high-frequency component signal relative to the deflection coil current signal may be noted.

Function  $S(\tau)$ , which is a result of secondary signal processing using the coherent accumulation method, describes the probability of excitation of high-frequency oscillations of plasma parameters. In addition, the probability of the exit of an electron from the keyhole affects the form of the function  $S$ .

#### 4 The Mechanism of Formation of a Secondary Signal in the Plasma

To explain the mechanism of the appearance of high-frequency oscillations in the secondary signal in the plasma we invoke two hypotheses.

The first deals with the assumption of the existence of explosive boiling in the keyhole [13, 14]. The rate of energy input in the interaction of the electron beam with the metal in the keyhole is much higher than the rate of energy output through

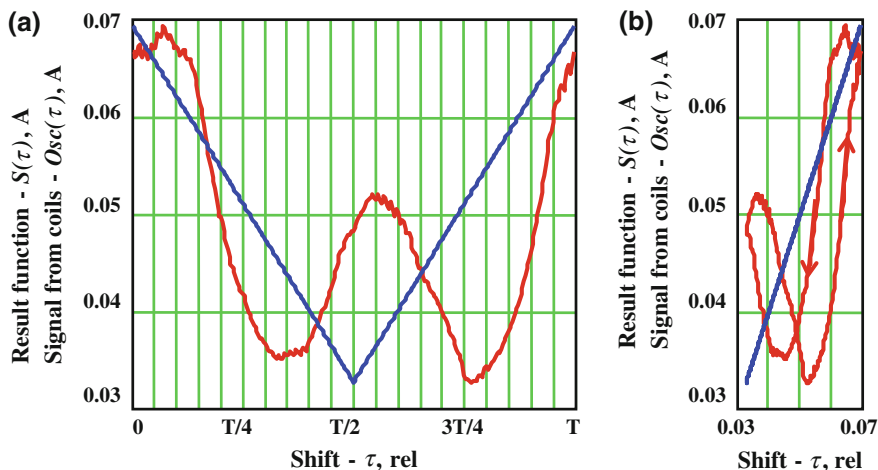


**Fig. 5** Function  $S(\tau)$ , obtained using the coherent accumulation method on  $\tau$ , is the result of secondary processing of the high-frequency component signal.  $Osc(\tau)$  is the record of the deflection coil current ( $P = 3$  kW, underfocused regime ( $\Delta I_f = -10$  mA), oscillation frequency  $f = 556$  Hz, sweep size  $2A = 1.5$  mm)

conduction. There is local overheating of the metal, followed by explosive boiling. The boiling metal vapor affects beam shielding: the beam is scattered by the metal vapor and the power density is dramatically reduced. After the vapor has been evacuated from the keyhole, the beam's power density again rises above the critical level and the process resumes.

We will estimate the order of the frequencies of the self-oscillating processes that the described hypothesis yields [17].

The process of overheating metal is usually considered first. The primary components of the energy balance look like this

$$q = q_v + q_m + q_c \quad (2)$$

where  $q$  is the power added by the beam,  $q_v$  is the heat loss due to vaporization,  $q_m$  is the heat loss due to melting, and  $q_c$  is the heat loss due to thermal conduction.

When moving the beam in the oscillation process into an already melted section the  $q_m$  term will not work. The vapor in the keyhole is similar to the saturated [18, 19]; the loss due to vaporization is considered to be no more than 5–10 %. When increasing the power density of the source  $q$ , sooner or later the rate of heat input will be much larger than the rate of heat discharge through thermal conduction. Moreover, the maximum energy release takes place at a certain depth below the border of the liquid metal at approximately the depth of the range of the electrons. The estimation is based on the characteristic energy accumulation time  $\tau_0$ , i.e. the time required to add enough energy for boiling. In the situation described, according to the theory of homogeneous boiling, if the energy accumulation time is comparable to or

less than the time of homogeneous nucleation, then overheating followed by explosive boiling are expected [20].

Disregarding the losses due to thermal conduction, the energy accumulation time may be obtained from the condition

$$\tau_0 = \frac{L_V \rho \delta}{q} \quad (3)$$

where  $L_V$  is the boiling heat and  $\rho$  is the density.

For stainless steel, given welding power  $P = 3$  kW and beam diameter  $d = 0.5$  mm, the energy accumulation time is  $\tau_0 \approx 2 \times 10^{-5}$  s. Moreover, the time will decrease with an increase in the power density, which indicates an increase in the likelihood of the occurrence of explosive boiling as the focus becomes sharp or when, all other things being equal, the welding power is increased.

The process of boiling is a phase transition and is accompanied by an expansion of the matter from an initial density of  $\sim 10^4$  kg/m<sup>3</sup> (liquid) to  $10^{-1}$  kg/m<sup>3</sup> (gas). Thus, after the matter boils, a layer of vapor appears in the electron beam's path with a particle concentration that rapidly falls from  $10^{26}$  to  $10^{20} - 10^{22}$  m<sup>-3</sup>.

It is well-known that when an electron beam passes through matter that there is an exponential attenuation in the beam's intensity due to energy being scattered and absorbed as a result of elastic and inelastic collisions. For example, in the case of absorption in a gaseous medium [21], the change in the beam's density is

$$j = j_0 \exp(-n\sigma x) \quad \text{or} \quad j = j_0 \exp(-\alpha \rho n x) \quad (4)$$

where  $n$  is the concentration of atoms in the vapor,  $\sigma$  is the interaction cross-section, and  $\alpha$  is the absorption factor.

Due to the fact that the vapor's initial density is high, we can expect shielding (scattering, defocusing) of the electron beam as a result of the interaction with the vapor particles. When the beam propagates vapor in the keyhole, the interaction is primarily elastic. Thus, we may suppose that the attenuation of the electron beam's intensity is related to the scattering of electrons outside of the action zone or on the keyhole walls. With a keyhole depth of  $H = 1.5$  cm, the energy flow density is attenuated by a factor of  $e$  given a concentration of  $n = 10^{25}$  m<sup>-3</sup>. The continuous action of the electron beam is periodically interrupted when the vapor's density exceeds a certain critical level. This self-oscillating process's time balance is the sum of the time for vaporization  $\tau_0$  and the vapor dispersion time  $\tau_v$ .

The simplest way to estimate  $\tau_v$  is to use sound wave propagation through the keyhole. Given  $H = 1.5$  cm and a sonic speed of 700 m/s, we obtain  $\tau_v \approx 2 \cdot 10^{-5}$  s.

The frequency of the "quasi-periodic" process becomes  $f = 1/\tau$  ( $\sim 25$  kHz), which agrees well with experimental data (Fig. 1) in terms of the order-of-magnitude. Similar estimates of the frequencies of the described process, which accompanies explosive boiling, have been independently obtained [13, 14, 17, 20, 22].

The conditions of the explosive rupture of metal on the front wall of the keyhole are determined by the pulsed nature of the emission of electrons from the electron beam's action area, which is related to the intense emission of an electron current when the metal transitions from a condensed state to a completely vapor-plasma phase. Estimating the current density of the thermionic emission using Richardson's equation demonstrates that when temperatures in the keyhole are on the order of the boiling temperature at the given pressure, overheating by 100 K leads to a doubling of the thermionic current. This is evidence of the high theoretical values of current emission into the plasma during electron beam welding using a powerfully concentrated electron beam. However, the actual current of a dependent discharge in the plasma during electron beam welding is determined by the current propagation conditions in the plasma and largely depends on the potential distribution in the plasma and external circuit's parameters.

Mladenov and Sabchevski [23] establishes the possibility of a self-oscillating process associated with periodic ionic self-focusing and defocusing. The electron beam's equilibrium radius is extremely dependent on the ion concentration in the keyhole. It causes the oscillatory nature of the electron beam's interaction with the metal. As the power of the electron beam increases above a critical value, the concentration of atoms increases sharply. The metal evaporates from the surface of the weld pool, creating the conditions for the development of noticeable ionic self-focusing of the electron beam. As the beam diameter decreases, the energy concentration increases, which causes a further increase in surface temperature and evaporation. Electron scattering is enhanced. The vapor concentration increases above a certain value and the beam size increases again. The subsequent decrease in temperature and loss of vapor again lead to the predominance of the self-focusing process, etc.

Uglov and Selishev [17] proposes to estimate the frequency of this process by using the electron beam neutralization time

$$\tau_i = (n_0 \sigma_i u)^{-1} \quad (5)$$

where  $n_0$  is the neutral gas's atom density,  $\sigma_i$  is the effective cross-section of the ionization of gas by the beam's electrons, and  $u$  is the speed of the beam's electrons. In the case of electron beam welding,  $\tau_i < 10^{-4}$  s. The characteristic frequency turns out to be close to the Langmuir ionic frequency and, under the conditions being considered, is greater than  $10^2$  kHz. Thus, the indicated process cannot be an independent cause of the mentioned oscillations. Furthermore, [24, 25] refute the very proposition of significant "self-compression" of the beam in a keyhole subjected to ionic focusing.

An analysis of all of the factors shows that the occurrence of high-frequency oscillations of the secondary current in the plasma may be related to the occurrence of the phenomenon of anomalous resistance of plasma [26–28]. Anomalous resistance of plasma is resistance that is associated with the development of various kinds of current instabilities and that occurs when the current density in the plasma exceeds a certain critical value. Anomalous resistance of plasma is only



related to hybrid electro-ionic instabilities and is substantially larger in magnitude than ordinary classical resistance due to paired electron-ion collisions. The critical current density  $j$  at which anomalous resistance occurs is usually expressed through a threshold value of electron drift velocity

$$V_d = j/n_e e. \quad (6)$$

In plasma without a magnetic field, people have spoken of the occurrence of ionic-sonic instability and the minimum value for the velocity  $V_d$  at which it occurs, which practically coincides with the velocity of ionic sound in plasma. Ionic-sonic instability is a build-up of longitudinal electrostatic oscillations in plasma with “hot” electrons and “cold” ions [29].

The speed of ionic sound in plasma depends only on the temperature of the electrons and the mass of the ions

$$V_s = \sqrt{\gamma k_b T_e / m_i}, \quad (7)$$

where  $k_b$  is Boltzmann’s constant,  $\gamma$  is the adiabatic index, and  $T_e$  is the temperature of the electrons. The temperature of the electrons over the zone of electron beam welding is on the order of 4,000 K [3]. In the experiments described, an electron collector with a voltage of  $\sim 50$  V creates an additional electric field in the plasma in the thin layer close to the cathode (a welding product). This electric field accelerates the electrons and their energy is then converted into thermal energy as a result of collisions with atoms and ions. Suppose that as a result of the described phenomenon the temperature rises to 14,000 K. Then the velocity of ionic-sonic waves is  $V_s \approx 1,650$  m/s.

Let us estimate the conditions under which ionic-sonic instability occurs ( $V_d = V_s$ ). In the experiments described, the strength of the secondary current in the plasma in pulses reaches magnitudes on the order of 1 A, given a collector diameter of 70 mm. Given these assumptions, ionic-sonic instability may occur if the concentration of electrons in the plasma over the welding zone does not exceed

$$n_e = \frac{j}{V_d e} = \frac{4I}{\pi D^2 V_d e} \sim 10^{18} \text{ m}^{-3}. \quad (8)$$

In the area where the electron collector is located, the concentration is known to be lower, and thus ionic-sonic instabilities are likely to occur.

For ionic-sonic oscillations, in the case of large wavelengths  $kr_{De} \ll 1$ , the dispersion relation takes the form of a linear dependence  $\omega(k) = kV_s$ , which is characteristic of sound waves ( $k$  is the wave number). If a consistent frequency and arbitrary velocities are typical for Langmuir ionic oscillations, then in ionic-sonic waves the speed is constant, but the frequencies may take on a wide range of values, depending on the wavelength. We will assume a wavelength equal to the typical size of the system (a working distance of 100 mm). In this case, the frequency turns out to be equal to  $f = V_s/\lambda \sim 16$  kHz. Of course, such good

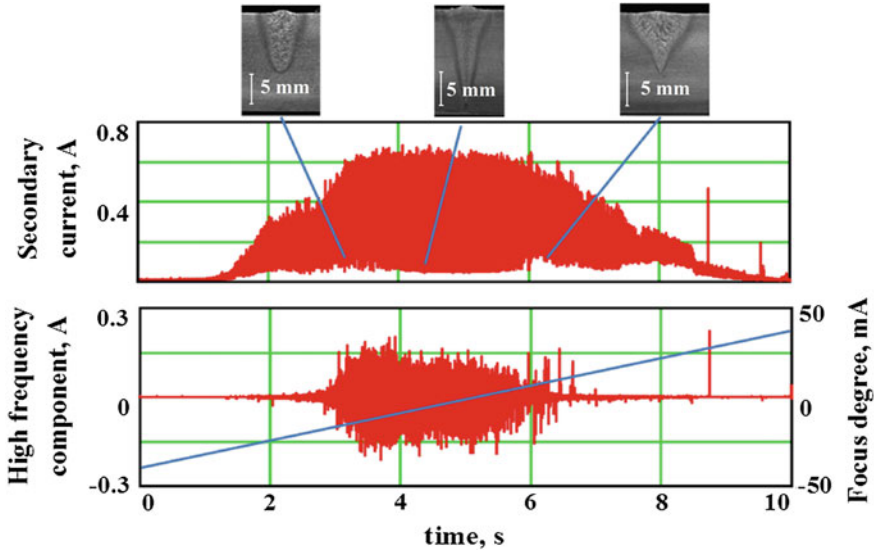


**Fig. 6** The high-frequency component of the secondary current during the linear rise of the focus coil current. ( $P = 2$  kW, oscillation frequency across the joint  $f = 556$  Hz, sweep size  $2$  A =  $1.5$  mm)

agreement with the experimentally observed spectrum (Fig. 1) is coincidental. The calculations presented only claim to estimate the order of magnitude.

In the context of the hypothesis described, the observed correlation between the amplitude of the high-frequency component and the focusing mode is obviously dependent upon the fact that the likelihood of the occurrence of ionic-sonic instability grows when the electron drift velocity (magnitude of the secondary current) increases. Given the occurrence of sufficiently large pulse in the secondary current, there is a “blockage” of the plasma gap as a result of anomalous resistance of plasma. The ionic-plasma instability increases and the long pulse of secondary current is interrupted in a series of high-frequency surges. This phenomenon is well-known in the physics of large magnitude pulsed discharges [30].

Thus, possible causes for the observed high-frequency oscillations in the “keyhole-plasma” system are: (a) oscillatory processes of the thermal field in the keyhole caused by the periodic explosive boiling and subsequent defocusing of the electron beam on the products of the discharge; (b) oscillatory ionic-sonic processes in the plasma over the welding zone. In either event, the likelihood of these processes grows with an increase in the thermionic emission from the welding area and thus characterizes the electron beam’s energy density.

Figure 6 shows the secondary current and the high-frequency component ( $f > 10$  kHz) during the linear rise of the focus coil current. The signal is appreciable in a certain range, accompanied by deep penetration. The high-frequency component appears in a narrow range. The dependence of the high-frequency

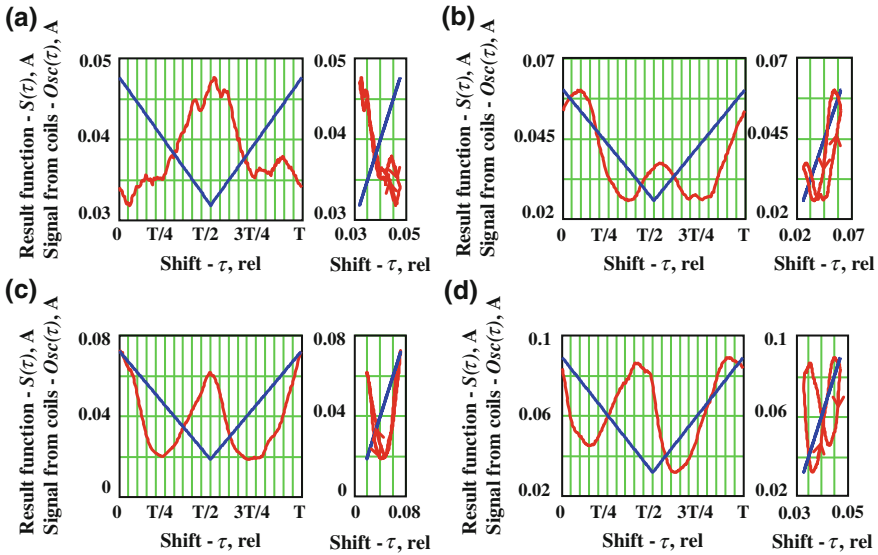


**Fig. 7** Function  $S(\tau)$ , obtained using the coherent accumulation method for the high-frequency component and  $Osc(t)$ , a record of the deflection coil current during welding along the joint. **a** Under-focused regime ( $\Delta I_f = -15$  mA); **b** under-focused regime ( $\Delta I_f = -7$  mA); **c** sharp focus regime ( $\Delta I_f = 0$  mA); **d** over-focused regime ( $\Delta I_f = 10$  mA); ( $P = 3$  kW, oscillation frequency  $f = 450$  Hz, sweep size  $2A = 1.5$  mm)

component on the power density (the focus degree) is used to construct operational control methods.

The assertion of the dependence of the probability of high-frequency oscillations on the density of the beam power allows interpretation of the results obtained by the coherent accumulation method for various focus regimes (Fig. 7).

For sharp-focus regimes with maximum penetration depth and over-focused regimes, the beam interacts with the front and back walls almost equally (Fig. 7c, d). The minimum of the high-frequency component signal in this position corresponds to the position at the bottom of the keyhole. The bottom of the keyhole practically coincides with the center of symmetry of the oscillating beam.

As the focus goes down (decreasing the current focus), the minimum of the function of the coherent accumulation method is shifted relative to the center of symmetry of the oscillation beam. This means that the bottom of the keyhole moves relative to the center of symmetry, and the electron beam begins to interact more with the front wall of the keyhole and less with the back one (Fig. 7b).

For strong under-focused regimes (Fig. 7a), when the formation of the keyhole is just beginning, the beam interacts with only the front wall of the keyhole. The high-frequency component signal is maximal at the moment of maximum electron-beam deflection against the welding direction. It appears that at this moment the beam interacts with the bottom of the keyhole. The minimum diameter of the electron beam in this case is below the bottom of the keyhole. Under these

conditions, the maximum power density of the electron beam is reached at the bottom of the keyhole. At the top of the keyhole, the power density is less critical, and high-frequency oscillations do not occur there.

We must note that we have still not fully explained the sharp decrease in the secondary current when lowering the area of interaction between the electron beam and the metal deep in the walls of the keyhole. It may be that this is related to the enormous current densities in the keyhole and, as a result, the continuously “blocked” state of the plasma there. It may be that in the keyhole the level of ionization is an order of magnitude less than expected, and the Debye radius is still larger than the lateral dimension of the keyhole. In this case, the plasma does not penetrate the keyhole. The interpretation of this phenomenon will be the subject of future research.

## 5 Conclusions

1. In this chapter, the ability to study processes in the keyhole (keyhole) during electron-beam welding was demonstrated. A combination of an application of beam deflection oscillation and an analysis of the instabilities of the secondary current in the plasma over the welded samples was used for this purpose.
2. The experimentally obtained secondary current signal in a plasma during electron-beam welding with electron beam oscillation contains a series of high-frequency perturbations, which follow each other at certain frequencies that are multiples of the deflection oscillation frequency.
3. It was shown that the probability of occurrence of these high-frequency perturbations increases with the concentration of energy in the interaction zone. Hypotheses for the emergence of high-frequency oscillating processes in the “beam-keyhole-plasma” structure were considered. Possible causes for the observed high-frequency oscillations in the “keyhole-plasma” system are: (a) oscillatory processes of the thermal field in the keyhole caused by the periodic explosive boiling and subsequent defocusing of the electron beam on the products of the discharge; (b) oscillatory ionic-sonic processes in the plasma over the welding zone. In either event, the likelihood of these processes grows with an increase in the thermionic emission from the welding area and thus characterizes the electron beam’s energy density.
4. It was established that during electron-beam welding in a not fully focused mode, the electron beam mainly interacts with the front side and the bottom of the keyhole. In sharp focusing and over-focused modes, the beam interacts practically in the same way with both the front and back sides of the keyhole.
5. It was established that during processing of the high-frequency part of the secondary current in a plasma using the coherent accumulation method, there is a lag of the high-frequency part of the signal in comparison with the deflection coil current signal. The degree of lagging decreases monotonically as the

focusing mode changed from an unfocused to over-focused state, and it is zero for the sharp focusing mode.

6. It must be noted that we have still not fully explained the sharp decrease in the secondary current when lowering the area of interaction between the electron beam and the metal deep in the walls of the keyhole. It may be that in the keyhole the level of ionization is an order of magnitude less than expected, and the Debye radius is still larger than the lateral dimension of the keyhole. In this case, the plasma does not penetrate the keyhole. The interpretation of this phenomenon will be the subject of future research.

**Acknowledgments** The authors would like to express their thanks to the Russian Foundation for Basic Research No 13-08-00397A and the Ministry of Education of Perm District of the Russian Federation for financial support.

## References

1. Chi CT, Chao CG, Liu TF, Wang CC (2008) Relational analysis between parameters and defects for electron beam welding of AZ-series magnesium alloys. *J Vac* 82:1177–1182
2. Babu NK, Ramana S, Murthy CV, Reddy GM (2007) Effect of beam oscillation on fatigue life of Ti–6Al–4V electron beam weldments. *J Mater Sci Eng* 471:113–119
3. Krinberg I, Mladenov G (2005) Formation and expansion of the plasma column under electron beam-metal interaction. *J Vac* 77–4:407–411
4. Trushnikov DN, Yazovskikh VM, Belenkiy VY (2007) Formation of a secondary-emission signal in electron beam welding with continuous penetration. *J Weld Int* 21–5:384–386
5. Griskey MC, Stenzel RL (1999) Secondary-electron-emission instability in a plasma. *J Phys Rev Lett* 82–3:556–559
6. Olszewskaa K, Friedel K (2004) Control of the electron beam active zone position in electron beam welding processes. *J Vac* 74:29–43
7. Yazovskikh VM, Trushnikov DN, Belenkiy VY (2004) The mechanism of secondary emission processes in electron beam welding with the modulation of the electron beam. *J Weld Int* 18–9:724–729
8. Trushnikov DN, Belenkiy VY, Mladenov GM, Portnov NS (2012) Secondary-emission signal for weld formation monitoring and control in electron beam welding. *J Materialwiss Werkstofftech* 43(10):892–897
9. Teng W, Xiangdong G, Katayama S, Xiaoli J (2012) Study of dynamic features of surface plasma in high-power disk laser welding. *J Plasma Sci Technol* 14–3:245–251
10. Kaplan AFH, Norman P, Eriksson I (2009) Analysis of the keyhole and weld pool dynamics by imaging evaluation and photodiode monitoring. In: Proceedings of LAMP2009, the 5th international congress on laser advanced materials processing, pp 1–6
11. Teresa S, Antonio A, Domenico R, Valentina L, Luigi T, Pietro M (2010) Plasma plume oscillations monitoring during laser welding of stainless steel by discrete wavelet transform application. *J Sensors* 10–4:3549–3561
12. Peng Y, Chen W, Wang C, Bao G, Tian Z (2001) Controlling the plasma of deep penetration laser welding to increase power efficiency. *J Phys D Appl Phys* 34–21:3145–3149
13. Rykalin, Uglov A, Zuev I, Kokora A (1985) Laser and electron beam treatment of materials. Mashinostroenie, Russia, Moscow (in Russian)

14. Smurov IY, Uglov AA, Lashyn AM, Matteazzi P, Covelli L, Tagliaferri V (1991) Modelling of pulse-periodic energy flow action on metallic materials. *J Int J Heat Mass Transf* 34:961–971
15. Trushnikov DN (2013) Using the wavelet analysis of secondary current signals for investigating and controlling electron beam welding. *J Weld Int* 27(6):460–465
16. Trushnikov D, Belenkiy V, Shchavlev V, Piskunov A, Abdullin A, Mladenov G (2012) Plasma charge current for controlling and monitoring electron beam welding with beam oscillation. *J Sensors* 12(12):17433–17445
17. Uglov AA, Selishev SV (1987) Autooscillation processes under the action of concentrated energy sources. Science, Russia
18. Kaplan A (1994) A model of deep penetration laser welding based on calculation of the keyhole profile. *J Phys D Appl Phys* 27:1805–1814
19. DebRoy T (1995) Physical processes in fusion welding. *Rev Mod Phys* 67–1:85–112
20. Skripov V, Sinitsyn E, Pavlov P, Ermakov G, Muratov G, Bulanov N, Baidakov V (1980) *Teplofizicheskie svoystva zhidkosti v metastabil'nom sostoyanii* (Thermophysical Properties of Liquids in Metastable State). Atomizdat, Moscow (in Russian)
21. Schumacher B (1964) A review of the (macroscopic) laws for electron penetration through matter. ORF
22. Belen'kii B (1979) The investigation of oscillation processes in the electron beam welding penetration channel. *Svar Proizvod* 8:6–7
23. Mladenov G, Sabchevski S (2001) Potential distribution and space-charge neutralization in technological intense electron beams—an overview. *J Vac* 62:113–122
24. Gabovich M, Simonenko L, Soloshenko I, Shkorina N (1974) Excitation of ion oscillations in plasma by a fast beam of negative ions. *Zh Eksp Teor Fiz* 67:1710–1716
25. Dilthey U, Goumeniouk A, Nazarenko O, Akopjantz K (2001) Mathematical simulation of the influence of ion-compensation, self-magnetic field and scattering on an electron beam during welding. *Vacuum* 62–2:87–96
26. Galeev A, Sagdeev R (1973) Nonlinear plasma theory. *Rev Plasma Phys.* Russia, Moscow (in Russian)
27. Kadomtsev V (1976) Collective phenomena in plasma. Russia, Moscow (in Russian)
28. Artsimovich A, Sagdeev R (1979) Plasma physics for physicists. Russia, Moscow (in Russian)
29. Akhiezer A (1974) Ion-acoustic oscillations. *Electrodynamics plasma.* Russia, Moscow (in Russian)
30. Chen F, Lieberman M (1984) Introduction to plasma physics and controlled fusion. Francis F: Plenum Press, New York